

Surface Stress, Kinetics, and Structure of Alkanethiol Self-Assembled Monolayers

Michel Godin,^{*,†} P. J. Williams,[‡] Vincent Tabard-Cossa,[†] Olivier Laroche,[†]
L. Y. Beaulieu,^{†,§} R. B. Lennox,^{||} and Peter Grütter[†]

Department of Physics, McGill University, Montreal, Quebec, Canada H3A 2T8, Department of Physics, Acadia University, Wolfville, Nova Scotia, Canada B0P 1X0, and Department of Chemistry, McGill University, Montreal, Quebec, Canada H3A 2K6

Received June 24, 2003. In Final Form: March 23, 2004

The surface stress induced during the formation of alkanethiol self-assembled monolayers (SAMs) on gold from the vapor phase was measured using a micromechanical cantilever-based chemical sensor. Simultaneous in situ thickness measurements were carried out using ellipsometry. Ex situ scanning tunneling microscopy was performed in air to ascertain the final monolayer structure. The evolution of the surface stress induced during coverage-dependent structural phase transitions reveals features not apparent in average ellipsometric thickness measurements. These results show that both the kinetics of SAM formation and the resulting SAM structure are strongly influenced both by the surface structure of the underlying gold substrate and by the impingement rate of the alkanethiol onto the gold surface. In particular, the adsorption onto gold surfaces having large, flat grains produces high-quality self-assembled monolayers. An induced compressive surface stress of 15.9 ± 0.6 N/m results when a $c(4 \times 2)$ dodecanethiol SAM forms on gold. However, the SAMs formed on small-grained gold are incomplete and an induced surface stress of only 0.51 ± 0.02 N/m results. The progression to a fully formed SAM whose alkyl chains adopt a vertical (standing-up) orientation is clearly inhibited in the case of a small-grained gold substrate and is promoted in the case of a large-grained gold substrate.

Introduction

Chemical self-assembly is increasingly being used for a multitude of applications including surface modification and functionalization. The idea of building structures from the bottom-up is one of the core concepts in nanoscience and promises to revolutionize many industries. For example, researchers in the field of molecular electronics are investigating the use of molecular self-assembly to build new types of transistors and switches that could replace today's dependence on silicon electronics.^{1–3} The drug industry is also interested in using the self-assembly principles to increase the efficiency of the drug delivery process.⁴ However, if self-assembly is to become a useful technology, it is important to understand the fundamental mechanisms that drive this process, from both a kinetics and structural point of view. This paper examines the kinetics of alkanethiol, $\text{HS}(\text{CH}_2)_n\text{CH}_3$, self-assembled monolayer (SAM) formation using simultaneous in situ surface stress and ellipsometric thickness measurements combined with ex situ STM imaging.

It is recognized that the formation of an alkanethiol SAM involves a sequence of several structural phase transitions.⁵ In the lower coverage regimes, this series of phases has a SAM structure defined by the alkanethiols

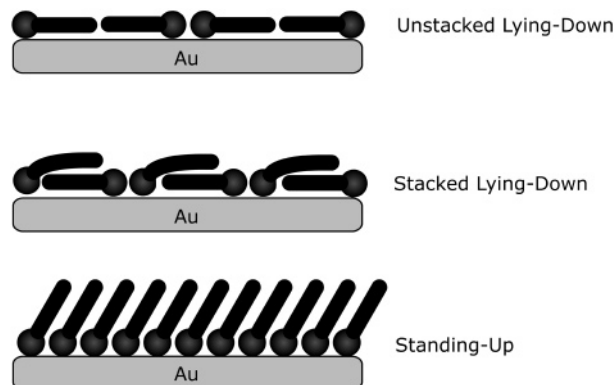


Figure 1. SAM formation is characterized by the transition from the lying-down phase to the stacked-lying phase before reaching the standing-up phase. The average alkanethiol film thickness increases with coverage. Other intermediate phases occur but are not depicted.

having their alkyl chains parallel to the Au surface (Figure 1). These lying-down (striped) phases coexist at modest coverage, while the transition into the standing-up phase occurs at greater coverage.

In a recent review paper, Schwartz⁶ lists several factors that influence the growth kinetics of alkanethiol SAMs. Many groups have observed that SAM formation occurs with two or more different time constants. Schreiber et al.,⁷ for example, observed a rapid process associated with the formation of the lying-down phases, followed by a second, much slower process governed by the transition into an ordered standing-up phase. Others propose that the transition into the standing-up phase can be ac-

* Corresponding author: e-mail, mgodin@physics.mcgill.ca.

[†] Department of Physics, McGill University

[‡] Department of Physics, Acadia University

[§] Present address: Memorial University, St. John's, NF, Canada A1B 3X7.

^{||} Department of Chemistry, McGill University.

(1) Heath, J. R.; Kuekes, P. J.; Snider, G. S.; Williams, R. S. *Science* **1998**, *280*, 1716.

(2) Reed, M. A.; Chen, J.; Rawlett, A. M.; Price, D. W.; Tour, J. M. *Appl. Phys. Lett.* **2001**, *78*, 3735.

(3) Diehl, M. R.; Yaliraki, S. N.; Beckman, R. A.; Barahona, M.; Heath, J. R. *Angew. Chem., Int. Ed.* **2002**, *41*, 353.

(4) Alper, J. *Science* **2002**, *296*, 838.

(5) Poirier, G. E. *Langmuir* **1999**, *15*, 1167.

(6) Schwartz, D. K. *Annu. Rev. Phys. Chem.* **2001**, *52*, 107.

(7) Schreiber, F.; Eberhardt, A.; Leung, T. Y. B.; Schwartz, P.; Wetterer, S. M.; Lavrich, D. J.; Berman, L.; Fenter, P.; Eisenberger, P.; Scoles, G. *Phys. Rev. B* **1998**, *57*, 12476.

accompanied or followed by a crystallization of the alkyl chains associated with molecular reorganization.^{8–13} The time constants associated with these formation processes are of particular relevance to the present study, as a discrepancy of up to 2 orders of magnitude in the time constants associated with SAM formation is observed for related experiments between laboratories.^{6–12} It is problematic to establish which part of the growth process (formation of lying-down phase, conversion to the standing-up phase, or some combination of the two) is being observed in SPR (surface plasmon resonance), QCM (quartz crystal microbalance), or spectroscopic measurements, for example. Complementary in situ experimental techniques are therefore needed to fully investigate the formation process.

In the present study, we show that we are able to track, in real time, alkanethiol SAM formation by measuring the induced surface stress. Simultaneous ellipsometric thickness measurements combined with ex situ STM imaging yields complementary information about the processes monitored by the surface stress measurement. In particular, we observe that the surface structure of the underlying gold substrate strongly influences both the kinetics of SAM formation and the resultant equilibrium SAM structure. Specifically, in the case of gold surfaces with small grain sizes (<100 nm), access to the high coverage, standing-up phase is inhibited. The impingement rate of the alkanethiols on the gold surface also strongly influences the final SAM structure. It is necessary that these two aspects be controlled if both the kinetics of alkanethiol SAM formation and the equilibrium structures are to be analyzed and compared.

Experimental Section

The kinetics of dodecanethiol¹⁴ ($\text{HS}(\text{CH}_2)_{11}\text{CH}_3$) adsorption from the vapor phase onto gold was investigated using three complementary techniques. The surface stress induced during SAM formation was measured in real time using a custom-made differential cantilever-based chemical sensor.¹⁵ Briefly, two atomic force microscope (AFM) cantilevers are positioned approximately 2 mm apart in a sealed aluminum cell. The cantilevers have been prepared by thermally evaporating gold onto one side of both cantilevers as described below. One cantilever is used as is, while the other is used as a reference. The reference cantilever is rendered inert to the presence of alkanethiols by predepositing a dodecanethiol SAM onto its surface. This SAM is formed by incubating the gold-coated reference cantilever in a 1 mM dodecanethiol/ethanol solution for 24 h. We found that the addition of the SAM to the reference cantilever does not significantly alter its spring constant. The reference cantilever is thus used to subtract unwanted signals resulting from variations in temperature and environmental noise. The deflection of both cantilevers is monitored using the optical beam deflection technique similar to that commonly used in AFM, as shown in Figure 2. The deflection of the gold-coated cantilever is directly proportional to the surface stress induced during monolayer formation.¹⁶ The measured cantilever deflec-

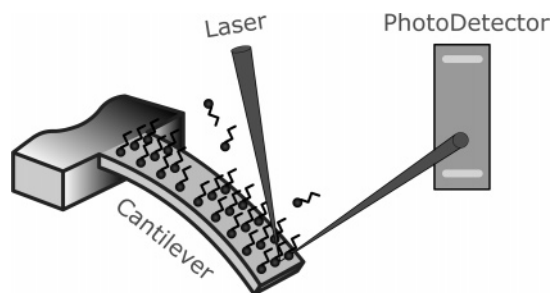


Figure 2. The optical beam deflection technique is used to monitor the induced deflection of the cantilever. The laser beam is reflected from the apex of the cantilever. The displacement of the reflected spot, which is proportional to the cantilever deflection, is monitored using a position-sensitive photodetector.

tion can be converted to a surface stress by additionally measuring the spring constant and geometry of the cantilever.^{17,18}

In a second system,¹⁵ a cantilever-based chemical sensor and an ellipsometer^{19,20} were combined to yield simultaneous surface stress and monolayer thickness measurements. In this case, gold-coated samples of mica²¹ (0.5 mm × 1.5 mm) were used for the ellipsometric measurements. Both cantilever and mica samples were placed in the same cell less than 1 mm apart to ensure identical adsorption conditions.

Dodecanethiol was introduced into both of these systems by injection through a Teflon-lined septum in pure liquid form. Liquid dodecanethiol (10–50 μL) was injected at a designated location in the closed cell. The dodecanethiol then evaporated into the vapor phase under ambient pressure, at room temperature, before reaching the gold-coated samples.

Scanning tunneling microscopy²² was used ex situ to image the resulting SAMs. Alkanethiol-covered samples were rinsed with anhydrous ethanol and blown dry with UHP nitrogen prior to imaging. All images were acquired in air, at constant current, using hand-cut $\text{Pt}_{80}\text{Ir}_{20}$ tips.²³

The gold films were prepared by thermal evaporation²⁴ at a base pressure of 1.0×10^{-5} Torr or lower. In this study, two types of gold surfaces were prepared: surfaces having a relatively small average grain size, and surfaces having a large average grain size. The small-grained gold surfaces were prepared by evaporating 10 nm of titanium²⁵ at a rate of 0.04 nm/s followed by 100 nm of gold²⁶ at a rate of 0.14 nm/s. These samples were not heated prior to the start of the evaporation, but radiative heating from the evaporation boats increased the sample temperature to $130 \pm 20^\circ\text{C}$. The large-grained gold was prepared by initially heating the silicon nitride, SiN_x (cantilever), and freshly cleaved mica substrates to $200 \pm 1^\circ\text{C}$ for 30 min. One hundred nanometers of gold was then evaporated at a rate of 0.14 nm/s. The heater was turned off during evaporation, but the substrate temperature reached $260 \pm 10^\circ\text{C}$ by the end of the evaporation. The sample temperature was kept under 300°C in order to prevent excessive permanent bending of the cantilevers. Although Ti was originally used as an adhesion layer, it was found that adequate adhesion was possible without it. All experiments were performed using freshly evaporated gold in order to minimize gold surface

(8) Bain, C. D.; Troughton, E. B.; Tao, Y.-T.; Evall, J.; Whitesides, G. M.; Nuzzo, R. G. *J. Am. Chem. Soc.* **1989**, *111*, 321.

(9) Grunze, M. *Phys. Scr.* **1993**, *T49B*, 711.

(10) Noh, J.; Hara, M. *Langmuir* **2001**, *17*, 7280.

(11) Noh, J.; Hara, M. *Langmuir* **2002**, *18*, 1953.

(12) Hähner, G.; Wöll, Ch.; Buck, M.; Grunze, M. *Langmuir* **1993**, *9*, 1955.

(13) Dannenberger, O.; Buck, M.; Grunze, M. *J. Phys. Chem. B* **1999**, *103*, 2202.

(14) Dodecanethiol from Sigma-Aldrich Canada; quoted purity 98+%, used as is.

(15) Godin, M.; Laroche, O.; Tabard-Cossa, V.; Beaulieu, L. Y.; Grütter, P.; Williams, P. J. *Rev. Sci. Instrum.* **2003**, *74*, 4902.

(16) Berger, R.; Delamarche, E.; Lang, H. P.; Gerber, Ch.; Gimzewski, J. K.; Meyer, E.; Güntherodt, H.-J. *Science* **1997**, *276*, 2021.

(17) Godin, M.; Tabard-Cossa, V.; Grütter, P.; Williams, P. *Appl. Phys. Lett.* **2001**, *79*, 551.

(18) The V-shaped cantilevers used were purchased from Thermo-Microscopes, California. Spring constants varied from 0.04 to 0.01 N/m for the 220–320 μm long cantilevers, respectively. Leg width and thickness for both cantilevers were 22 μm and 600 nm, respectively.

(19) Laroche, O. M.Sc. Thesis, McGill University, Montreal, Quebec, Canada, 2002.

(20) Gaertner Scientific, model L116C. The ellipsometer laser used had a wavelength of 632.5 nm and an angle of incidence of 70° . A constant index of refraction of 1.459 was used for dodecanethiol SAM thickness determination.

(21) V-4 grade mica was purchased from SPI Supplies, PA. Mica substrates were freshly cleaved prior to evaporation.

(22) Digital Instruments, USA.

(23) Goodfellow Cambridge Limited, U.K.

(24) Thermionics Laboratory Inc., USA, model VE-90.

(25) Alfa Aesar, CAN, 99.995% purity.

(26) Angstrom Sciences, USA, 99.99% purity.

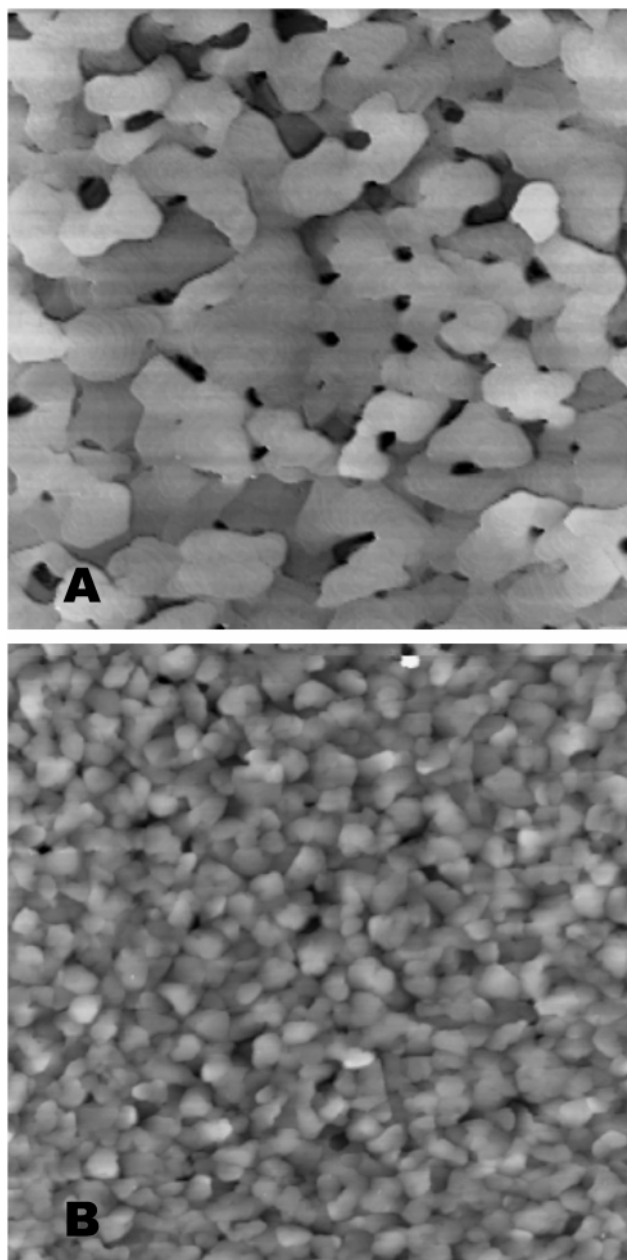


Figure 3. STM images ($3\ \mu\text{m} \times 3\ \mu\text{m}$) of (A) large-grained gold and (B) small-grained gold. Images were acquired in air with a tip bias of 600 mV and tunneling current of 35 pA. Height contrast scale is 14 nm for both images.

contamination due to exposure to air, which affects SAM formation.

Results and Discussion

Figure 3 shows STM images (acquired in air) of the two gold surfaces used in these studies. Figure 3A shows gold with large grains, whereas Figure 3B reveals gold having much smaller grains. The large grains had an average size of 600 ± 400 nm, while the small grains had an average size of 90 ± 50 nm. The root mean square roughnesses of the gold in Figure 3A and Figure 3B are 0.3 ± 0.1 and 0.9 ± 0.2 nm, respectively, on a 200 nm length scale. X-ray diffraction reveals that both the large- and small-grained gold are highly ordered Au(111). It should be noted that STM verifies that the gold prepared concurrently on both the mica surface (for the ellipsometry studies) and on the SiN_x cantilever surface (for the cantilever-based stress sensor) was similar, in terms of grain size and roughness.

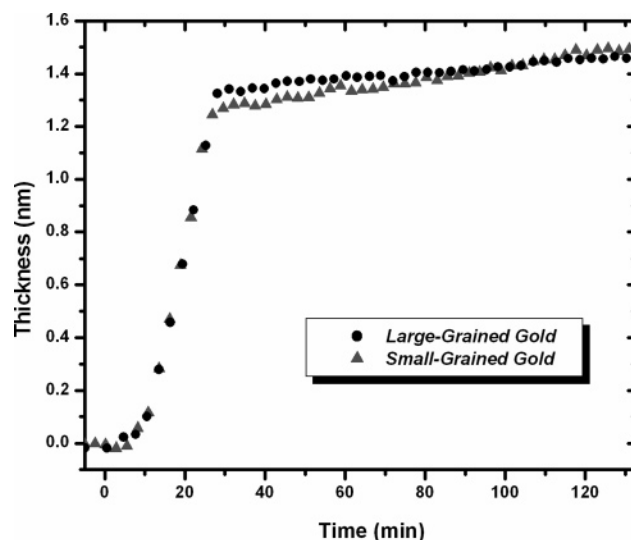


Figure 4. Real-time thickness profiles of the dodecanethiol SAMs grown on small- and large-grained gold. Dodecanethiol was introduced at time $t = 0$ min.

Simultaneous in situ surface stress and thickness measurements were performed as a function of time, on both large- and small-grained gold. Figure 4 shows that the real-time average thickness profiles of the dodecanethiol SAMs, as they grow on the two types of gold, are fairly similar. Each SAM reaches an average thickness²⁷ of 1.5 ± 0.1 nm within approximately 120 min. Ellipsometry therefore does not suggest that there are any significant differences between the two gold surfaces in terms of adsorption kinetics or final SAM structure. However, simultaneous surface stress measurements reveal that the SAMs formed on these two gold surfaces are indeed very different, as shown in Figure 5. The deflection signals of the reference cantilevers (not shown) show negligible deflection when exposed to dodecanethiol vapor, as compared to the measured deflections of the active cantilevers. The surface stress curves are thus due only to the compressive (i.e., cantilever bends away from the gold-coated side) surface stress induced during alkanethiol adsorption. Both the small- and large-grained gold exhibit an initial rapid development of the surface stress, reaching a value of approximately 0.4–0.6 N/m after 2.5 min (Figure 5B). This initial increase in surface stress is more rapid for the large-grained gold, and a slightly larger surface stress is measured at this time. The long-term evolution of the surface stress is, however, markedly different for the two systems (Figure 5A). The surface stress on the large-grained gold continues to increase for approximately 10 h, reaching a final value of approximately 16 N/m, while the small-grained gold exhibits only a slight increase in surface stress, reaching a final value of approximately 0.5 N/m in minutes. We turned to the direct STM imaging of the SAMs formed on the small- and the large-grained gold to probe the origins of this puzzling difference between ellipsometric thickness/time and surface stress/time profiles.

Ex situ molecular resolution STM imaging was performed to survey the structure of the resulting SAM. Although a survey of the entire gold surface was not possible, it was found that the SAM resulting from adsorption onto the large-grained gold is fully in a standing-up phase, as shown in the STM image ($44.7\ \text{nm} \times 44.7\ \text{nm}$) of Figure 6A, where the $(\sqrt{3} \times \sqrt{3})\text{R}30^\circ$ structure and its $c(4 \times 2)$ superlattice are observed in

(27) The resolution of the ellipsometric measurement was 0.1 nm.

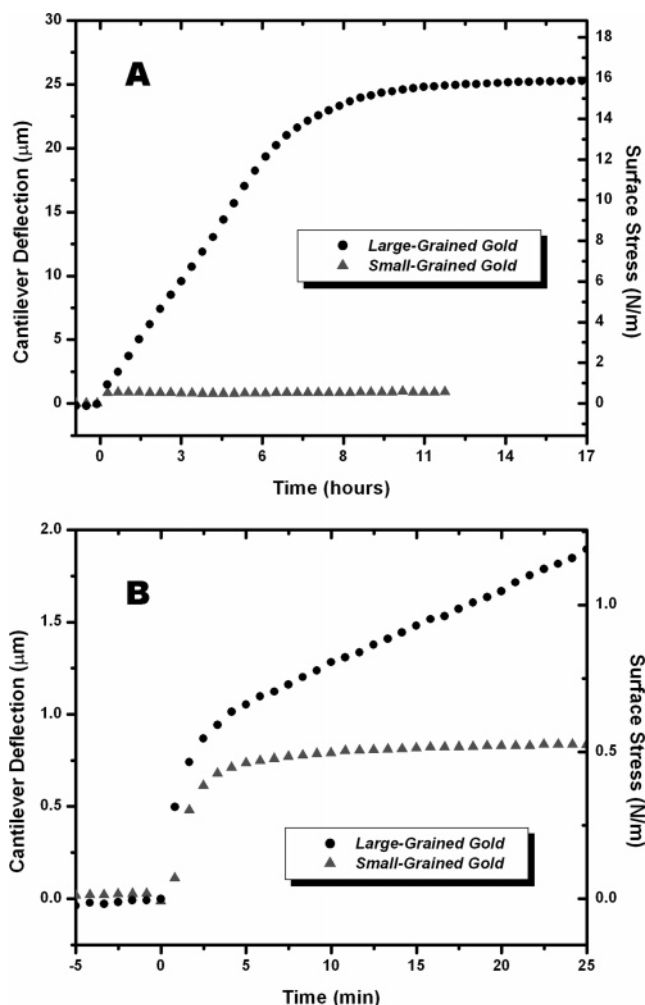


Figure 5. The surface stress induced during the formation of dodecanethiol SAM on gold-coated cantilevers. (A) The SAM grown on large-grained gold exhibits a long-term increase in surface stress, which is not observed for the SAM grown on small-grained gold. In both cases, the surface stress is compressive. Dodecanethiol was introduced at time $t = 0$ h. The first 25 min of SAM formation is shown in (B).

several adjacent domains. The dark surface features found (Figure 6A) are etch pits, which commonly result from alkanethiol adsorption on gold.^{28–30} Figure 6B is a zoom (7.9 nm \times 7.9 nm) of the boxed region of Figure 6A, clearly showing the $c(4 \times 2)$ superlattice of the $(\sqrt{3} \times \sqrt{3})R30^\circ$ lattice.³¹ The equivalent primitive unit cell $p(3 \times 2\sqrt{3})$, is also shown.

Figure 7 shows a STM image of the SAM grown on small-grained gold. In this case, alkanethiol domains of the lying-down phase coexist with domains of the standing-up phase. Although the standing-up phase is observed, a broad survey of the surface reveals that the lying-down phase is predominant. The spacing between the lying-down stripes is approximately 1.5 nm, consistent with a striped lying-down phase whose alkyl chains form an interdigitated bilayer on the gold surface; the result is a stacked lying-down phase.⁵ The measured average ellipsometric thickness for this situation is 1.5 ± 0.1 nm. It is

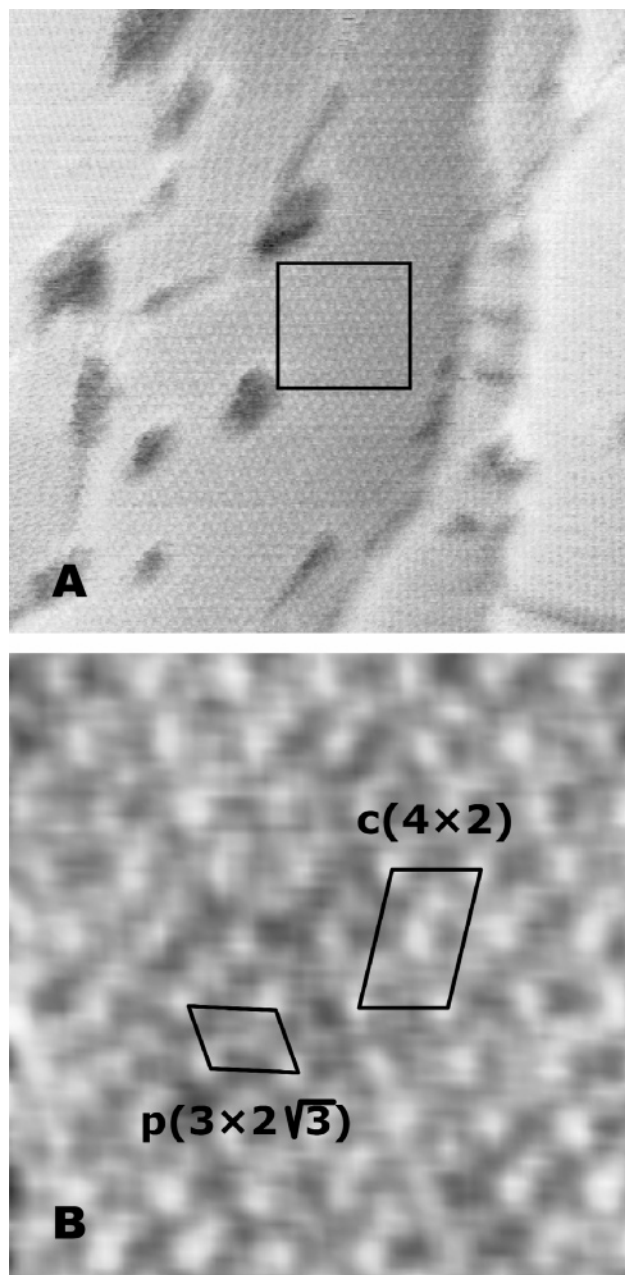


Figure 6. STM image (44.7 nm \times 44.7 nm) of a dodecanethiol SAM on gold. All alkanethiol domains present in (A) are in the standing-up phase. The middle domains exhibit the $c(4 \times 2)$ superlattice of the $(\sqrt{3} \times \sqrt{3})R30^\circ$ lattice. The domains in the upper left and on the right of the image show the $(\sqrt{3} \times \sqrt{3})R30^\circ$ configuration. A zoom (7.9 nm \times 7.9 nm) of part of the middle domain (boxed region) is shown in (B) and reveals the $c(4 \times 2)$ superlattice. The $p(3 \times 2\sqrt{3})$ primitive unit cell (0.85 nm \times 1.01 nm) is also shown. The STM tip bias was 600 mV, and the current was 25 pA.

interesting to note that although STM reveals that this is a mixture of stacked lying-down and standing-up phases, a thickness of 1.5 nm corresponds to the thickness of the fully standing-up dodecanethiol SAM.³² STM reveals the differences in the resulting SAM structure for formation on small- and large-grained gold, whereas the ellipsometric profiles of Figure 4 alone are insufficient for distinguishing the two cases.

These STM data thus help to resolve the origin of what appear to be very different time courses of ellipsometric

(28) Poirier, G. E. *Langmuir* **1997**, *13*, 2019.

(29) Dishner, M. H.; Hemminger, J. C.; Feher, F. J. *Langmuir* **1997**, *13*, 2318.

(30) Edinger, K.; Grunze, M.; Wöll, Ch. *Ber. Bunsen-Ges. Phys. Chem.* **1997**, *101*, 1811.

(31) Delamarche, E.; Michel, B.; Gerber, Ch.; Anselmetti, D.; Güntherodt, H.-J.; Wolf, H.; Ringsdorf, H. *Langmuir* **1994**, *10*, 2869.

(32) Meuse, C. W. *Langmuir* **2000**, *16*, 9483.

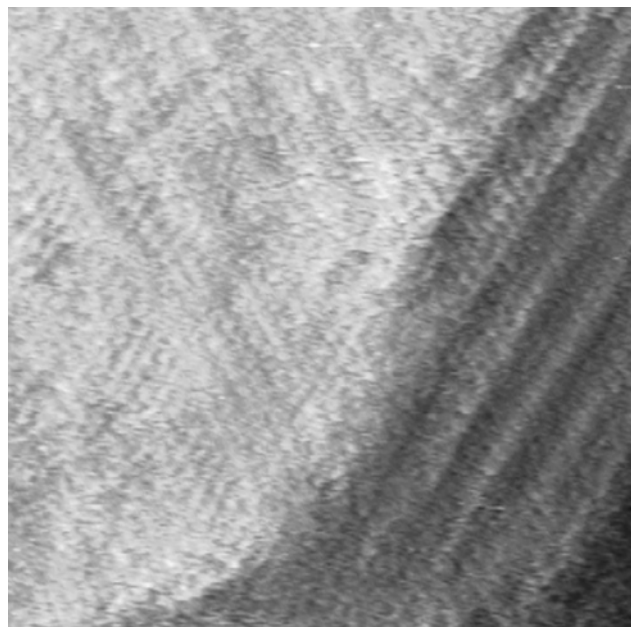


Figure 7. STM image ($24.5 \text{ nm} \times 24.5 \text{ nm}$) of mixed phases of dodecanethiol SAM on small-grained gold. The domain on the left side of the image exhibits a periodicity of 0.5 nm , indicating that the SAM is in the $(\sqrt{3} \times \sqrt{3})R30^\circ$ standing-up phase. The larger stripes on the lower right side of the image are spaced by 1.5 nm , typical of a stacked lying-down phase. The STM tip bias was 600 mV , and the current was 25 pA .

thickness and surface stress data. Single wavelength ellipsometry of course has limitations in making definitive assignment of thicknesses. First, variations in film index of refraction from the bulk value during the self-assembly process (for different phases)³³ can lead to a systematic error in thickness values, especially at low coverage. Second, the thickness value is a weighted average of the thickness of the different phases present. This is important because the SAM formed on small-grained gold, being predominately in the stacked lying-down state, clearly coexists with a measurable standing-up component. Any absolute differences between the thickness of dodecanethiol in the standing-up and lying-down states are therefore averaged in the ellipsometry experiment. STM, on the other hand, establishes that there are indeed important differences in the SAM formed on the two gold surfaces and that there is both greater alkanethiol coverage and order on large-grained gold compared to small-grained gold substrates.

The final surface stress values³⁴ were 0.51 ± 0.02 and $15.9 \pm 0.6 \text{ N/m}$ for SAM formation on small- and large-grained gold, respectively (Figure 5). The STM results strongly suggest that the large surface stress values measured on large-grained gold are due to the formation of highly ordered dodecanethiol SAMs adopting the $c(4 \times 2)$ structure. Previous reports of surface stress^{16,35,36} for dodecanethiol SAM formation from the vapor phase are consistent with the results obtained in this study for the

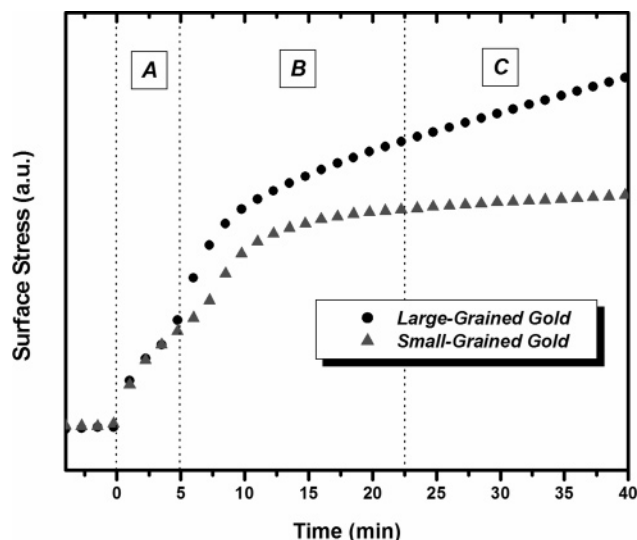


Figure 8. Initial stages of the surface stress profiles for dodecanethiol adsorption on large- and small-grained gold. The region labeled A corresponds to the initial stages of alkanethiol adsorption. Region B is associated with the transition into the lying-down phases. In region C, the transition into the standing-up phase begins for the adsorption onto the large-grained gold, whereas the SAM remains in a stacked lying-down phase for the small-grained gold.

small-grained gold. The STM images suggest that the SAMs formed on the small-grained gold do not achieve the highly ordered $c(4 \times 2)$ structure because progression to the requisite full coverage state is inhibited. Nevertheless, although the qualitative nature of the surface stress curves was quite reproducible, some variability remains in the quantitative measurement of the surface stress induced by SAM formation on large-grained gold. Sample-to-sample variations in the gold substrate structure might account for some degree of variability.

Figure 8 shows the initial stages of the induced surface stress for an experiment similar to the one depicted in Figure 5. The only difference here is that the growth was slowed by slightly increasing the separation distance between the liquid dodecanethiol droplet and the gold-coated samples.¹⁵ As a result, three distinct regions are now clearly resolvable in the surface stress curves associated with different stages of SAM formation. These features are also present in the data shown in Figure 5 but are less pronounced. On the basis of STM and ellipsometric results, we infer that region A in Figure 8 is associated with a disordered phase present at the early stages of alkanethiol adsorption. The process in region B is associated with transitions into the lying-down striped phases. In region C, the surface stress induced on the cantilever coated with large-grained gold continues to increase over a long time frame. This long-term increase in stress is related to the transition into the standing-up phase and its subsequent ordering. For adsorption onto small-grained gold, the surface stress ceases to increase since the SAM remains in a relatively low coverage state, where the stacked lying-down striped phase is predominant, but coexists with a few domains in the standing-up phase. The time constants associated with these different regions are a function of various factors, including cell geometry (i.e., vapor concentration), alkanethiol length, and gold cleanliness. Nevertheless, the time constant associated with the final process is always at least an order of magnitude larger than that of the first two processes. The features and transitions that appear in the surface stress profile are not readily identifiable in

(33) Peterlinz, K. A.; Georgiadis, R. *Langmuir* **1996**, *12*, 4731.

(34) The calculation of the surface stress from the cantilever deflection measurement involves an uncertainty of approximately 4%, or 0.6 N/m and 0.02 N/m for large- and small-grained gold, respectively (see ref 17). The standard deviations of the measured surface stress values in the last hour of each measurement (stability), when the surface stress profile reaches equilibrium, are 0.01 and 0.03 N/m for large- and small-grained gold, respectively.

(35) Berger, R.; Delamarche, E.; Lang, H. P.; Gerber, Ch.; Gimzewski, J. K.; Meyer, E.; Güntherodt, H.-J. *Appl. Phys. A* **1998**, *66*, S55.

(36) Hansen, A. G.; Mortensen, M. W.; Andersen, J. E. T.; Ulstrup, J.; Kühle, A.; Garnæs, J.; Boisen, A. *Probe Microsc.* **2001**, *2*, 139.

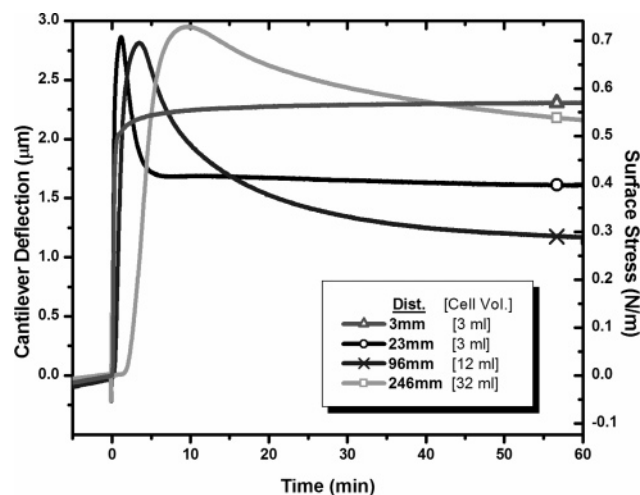


Figure 9. Surface stress profiles for various alkanethiol droplet/cantilever distances. For distances of 23 mm or greater, a maximum in the surface stress (stress release) is observed, and the final average SAM thickness reaches 0.7 ± 0.1 nm.

the ellipsometric profile of Figure 4. However, although the average ellipsometric thickness profiles (e.g., Figure 4) did not always distinguish features in a multistep process, they also did not follow simple Langmuir kinetics, as observed in other ellipsometric studies.³⁷ On the basis of simultaneous surface stress measurements, and *ex situ* STM imaging, we infer that the rapid increase (~ 30 min) in ellipsometric thickness in the profiles of Figure 4 is associated with the formation of the stacked lying-down phase. After 30 min, ellipsometry fails to identify the differences in SAM structure for formation on the two types of gold.

The dodecanethiol vapor concentration in the early stages of SAM formation also has a strong influence on the evolution of the surface stress induced during SAM growth. In the following series of experiments, the vapor deposition of dodecanethiol on gold-coated cantilevers was performed by injecting $150 \mu\text{L}$ of pure liquid dodecanethiol into a closed cell. Part of the liquid droplet then evaporated into the cell, and the alkanethiol vapor concentration increased to saturation in the vicinity of the gold surface. It should be noted that varying the volume of liquid alkanethiol injected into the cell did not affect the observed surface stress curves, as long as sufficient liquid was injected such that some remained in the cell when the vapor reached saturation. The time constant associated with this increase in concentration up to saturation is proportional to the square of the separation distance between the alkanethiol droplet and the cantilevers. As the SAM formed on the gold-coated cantilevers, the induced surface stress was measured as a function of time for different distances and cell volumes. This set of experiments was conducted on small-grained gold.

Figure 9 shows the induced surface stress as a function of time for alkanethiol droplet/cantilever separations of 3, 23, 96, and 246 mm, corresponding to cell volumes of 3, 3, 12, and 32 mL, respectively. Note that the shape of the kinetics curves is quite different for distances of 3 and 23 mm, although the volumes are the same. These two experiments were performed in the same cell, but the dodecanethiol droplet was injected at different places in the cell. These results clearly indicate that SAM formation is strongly influenced by the vapor concentration in the early stages of exposure. The development of the surface

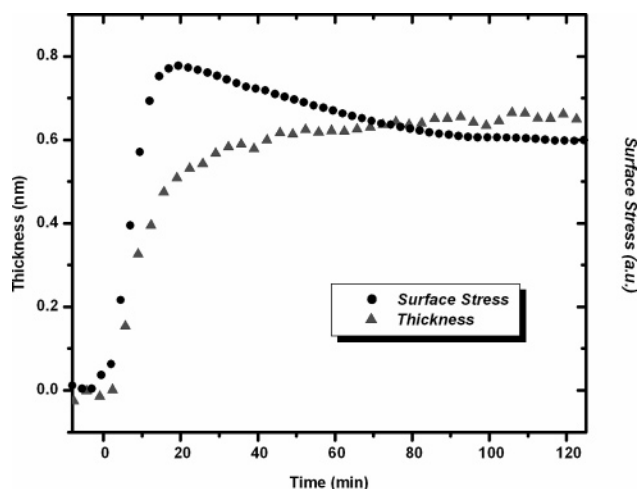


Figure 10. Simultaneous surface stress and ellipsometric thickness measurements of a SAM grown with an initially low vapor concentration. The surface stress curve exhibits a maximum (stress release), while the ellipsometric thickness monotonically increases, attaining an eventual value of 0.7 ± 0.1 nm.

stress occurs over longer time scales, indicating that the growth is diffusion limited. We also observe that the surface stress curves exhibit a stress release (i.e., maximum in the stress signal) for large droplet/cantilever distances. In these cases, ellipsometry reveals that the resultant SAM attains only partial monolayer coverage. Figure 10 shows that the final average thickness reaches 0.7 ± 0.1 nm, instead of the 1.5 ± 0.1 nm associated with either that expected for a fully standing-up, or a stacked lying-down, SAM. We infer that a thickness of 0.7 ± 0.1 nm is consistent with alkanethiol adsorption leading to a lying-down phase whose alkyl chains are not stacked.^{5,38} The thickness of an unstacked lying-down domain previously measured by AFM (0.50 ± 0.05 nm)³⁸ is in the same range (but is smaller) as the 0.7 ± 0.1 nm average thickness measured here using ellipsometry. Notwithstanding the caveats surrounding the ellipsometric thickness values, the requisite compressive load of the tip in the AFM experiment introduces another type of uncertainty in thickness determination. We caution here that the interpretation of the ellipsometric thickness measurement (because of a phase-dependent index of refraction, and of thickness averaging for mixed phases, as discussed above) during alkanethiol SAM formation remains highly non-trivial. The use of complementary techniques in monitoring monolayer formation is essential in understanding the many mechanisms that drive the self-assembly process.

The structure of a SAM grown on small-grained gold also depends on the growth rate. For rapid growth rates, STM images (and supportive ellipsometry data) indicate that the final phase is a stacked lying-down phase. For slow growth rates, ellipsometry suggests that the final phase is an unstacked lying-down phase. The surface stress results are consistent with this interpretation, as the final stress value measured under conditions of slow growth (unstacked lying-down phase; stress release) is typically smaller than the final stress value measured in the rapid growth regime (stacked lying-down phase; no stress release). One would indeed expect that the induced surface stress would be larger for systems whose molecular

(37) Thomas, R. C.; Sun, L.; Crooks, R. M.; Ricco, A. J. *Langmuir* **1991**, 7, 620.

(38) Xu, S.; Cruchon-Dupeyrat, J. N.; Garno, J. C.; Liu, G.-Y.; Jennings, G. K.; Yong, T.-H.; Laibinis, P. E. *J. Chem. Phys.* **1998**, 108, 5002.

density is higher. It is possible that the molecular adsorption becomes slowed to the point that unstacked lying-down domains grow and achieve an energetically metastable state. Such a kinetically trapped state³⁹ is more prevalent for vapor phase deposition than for SAM formation from solution. For rapid growth, this intermediate state is not as stable and the transition of this metastable state into a denser, stacked lying-down phase is possible.

Summary

STM imaging of SAMs grown on large-grained gold revealed the presence of the $c(4 \times 2)$ superstructure of the $(\sqrt{3} \times \sqrt{3})R30^\circ$ lattice, which is consistent with a crystallized dodecanethiol SAM in the standing-up phase. An average final monolayer (ellipsometric) thickness of 1.5 ± 0.1 nm is consistent with the thickness of a dodecanethiol SAM in the standing-up phase. Adsorption onto small-grained gold resulted in a lower coverage, mixed phase SAM. In this case, STM imaging revealed that most domains were in a stacked lying-down phase, coexisting with some domains in the standing-up phase. While ellipsometry can be sensitive to phase transitions during SAM formation, STM must be used for phase identification. The large differences in surface stress response observed during alkanethiol adsorption onto small- and large-grained gold thus closely correlates with the difference in alkanethiol coverage and related SAM structure observed on these two substrates.

Three distinct processes are clearly resolved in the surface stress measurements, as outlined in Figure 8. The first two processes are associated with the formation of an initially disordered phase and a transition into a striped phase. The third is a long-term process where the large increase in surface stress is due to additional alkanethiol adsorption and the conversion of the striped lying-down phases into the standing-up phase. On small-grained gold, alkanethiol domains of the lying-down phase form, but their growth is inhibited in some fashion, so that a full conversion into the standing-up phase does not occur. The result is that the SAM remains in this state (stacked lying-down, with a small component in the standing-up phase), unable to undergo the full transition into the standing-up phase. We note that the average size of atomically flat areas available for SAM formation on the small-grained gold is of the same order of magnitude as typical domain sizes (~ 10 nm) that are observed for well-ordered

SAMs.^{40,41} Some STM studies⁵ suggest it is energetically favorable for the nucleation of the standing-up phase to occur at domain boundaries of the lying-down phase, through the so-called disordered liquid phase. We speculate that a certain number of adjacent domains (domain boundaries) of the lying-down phase are required to trigger nucleation of the standing-up phase. On small-grained gold, such nucleation sites are scarce. We stress that the mechanisms detailing the interplay between gold grain size and the phase transitions occurring during SAM formation are complex and remain to be fully understood. As for SAMs that are slowly grown on the small-grained gold, ellipsometry reveals a final SAM thickness of 0.7 ± 0.1 nm and is assumed to be a SAM in an unstacked lying-down phase.

Several factors are critical in SAM growth, such as temperature, substrate cleanliness, and others outlined in Schwartz's review.⁶ In this work, we have investigated two factors that have a strong influence on the growth of alkanethiol SAMs on gold: the underlying gold substrate structure and the alkanethiol vapor introduction conditions. Careful control and characterization of these factors are essential in order to obtain reproducible results. Despite careful control over many of these factors, we find that the surface stress measurement proves to be extremely sensitive to SAM growth conditions. Nevertheless, an understanding of the origins of the surface stress^{16,42} induced during the formation of alkanethiol SAMs will lead to a greater understanding of the mechanisms that drive the self-assembly process. Ongoing research is aimed at modeling the surface stress associated with SAM formation for comparison with experimental measurements.

Acknowledgment. We acknowledge the support of the Natural Sciences and Engineering Research Council of Canada (NSERC). M.G. thanks Le Fonds Québécois de la Recherche sur la Nature et les Technologies (FQRNT) for support through a doctoral fellowship. M.G. and V.T.-C. would additionally like to acknowledge the financial support given by McGill University through its McGill Major Fellowship program. L.Y.B. thanks NSERC for financial support through a postdoctoral fellowship.

LA030257L

(40) Poirier, G. E. *Chem. Rev.* **1997**, *97*, 1117.

(41) Kawasaki, M.; Sato, T.; Tanaka, T.; Takao, K. *Langmuir* **2000**, *16*, 1719.

(42) Fitts, W. P.; White, J. M.; Poirier, G. E. *Langmuir* **2002**, *18*, 1561.

(39) Schreiber, F. *Prog. Surf. Sci.* **2000**, *65*, 151–256.